IEEE Access
Multidisciplinary | Rapid Review | Open Access Journal

Received August 31, 2017, accepted September 24, 2017, date of publication September 29, 2017,
date of current version October 25, 2017.

Digital Object Identifier 10.1109/ACCESS.2017.2757949

Reconfigurable MIMO Antenna for Integrated-Metal-Rimmed Smartphone Applications

ZI-QIANG XU[1], (Member, IEEE), YANG-TAO SUN[1], QIANG-QIANG ZHOU[1], YONG-LING BAN[2], YUAN-XUN LI[1], AND SIMON S. ANG[3], (Fellow, IEEE)

[1]School of Energy Science and Engineering, University of Electronic Science and Technology of China, Chengdu 611731, China
[2]School of Electronic Engineering, University of Electronic Science and Technology of China, Chengdu 611731, China
[3]High Density Electronics Center, University of Arkansas, Fayetteville, AR 72701 USA

Corresponding authors: Zi-Qiang Xu (nanterxu@uestc.edu.cn) and Yong-Ling Ban (byl@uestc.edu.cn)

This work was supported in part by the National Natural Science Foundation of China under Grant 61301052 and Grant 61471098, in part by the Sichuan Science and Technology Support Projects under Grant 2017GZ0106, Grant 2017GZ0143, and Grant 2017GZ0200, and in part by the Fundamental Research Funds for the Central Universities of China under Grant ZYGX2015J095, Grant 2016J035, and Grant 2016J145.

ABSTRACT A reconfigurable full-metal-rimmed MIMO antenna is designed and proposed for WWAN/LTE smartphones. This antenna consists of two centro-symmetrically distributed antenna elements and radiation structures using the unbroken metal rim in plastic casing. It can achieve a good isolation of more than 17dB over the entire operation bands. Each antenna element occupies a small ground area of 30×6 mm^2. The U-shaped feeding line provides a coupled feed and the antenna element generates four typical loop resonant modes. Using reconfigurable technique to combine these four resonant modes, this hepta-band MIMO antenna can satisfactory cover lower bands of GSM850/900 and higher bands of GSM1800/1900/ UMTS/LTE2300/2500. A prototype MIMO antenna was fabricated and the measured results of S-parameters, antenna efficiency and gain, envelope correlation coefficient, mean effective gain, and channel capacity are reported.

INDEX TERMS Reconfiguration, MIMO, integrated-metal rim, WWAN/LTE, antenna.

I. INTRODUCTION

Multiband smartphones with a metal rim are becoming popular in recent years [1]. Compared with a plastic casing, the metal rim is both stylistically appealing and functionally able to increase its mechanical robustness. However, undesired mutual coupling occurs between the inner antenna and outer metal rim can seriously degrade the performance of the smartphone antenna. This problem poses a great challenge to designing multi-band smartphone antenna with integrated-metal rim. Several promising solutions were proposed to alleviate the deleterious effects of metal rim [2]–[7]. One common method [2]–[5] is to introduce multiple gaps into the outer metal rim. While this method can effectively reduce the negative impact on the performance of the inner antennas, the strength of the metal-rimmed plastic casing and perfect configuration of metal rim are significantly affected. Nevertheless, loop antennas capable of generating multiple resonant modes [8]–[10] are good candidates for the unbroken metal-rimmed antenna in which the outer metal rim can function as a partial radiation structure [6], [7]. In [6], an unbroken metal-rimmed dual-loop antenna for smartphone applications is proposed. By merging multiple loop modes, seven WWAN/LTE bands can be achieved. However, the entire volume around the housing is occupied by the main antenna, leaving no space for other antennas in the smartphone. To further save space and achieve enhanced bandwidth, numerous techniques such as coupling feeding [11] and reconfigurable operating [12]–[16] are widely studied. In [12], a reconfigurable loop antenna with two parasitic grounded strips for unbroken metal-rimmed smartphones is investigated. Using reconfigurable technique, the antenna can cover the WWAN/LTE operating bands in a compact size.

With the rapid development of electronic communication, multiple antennas are desired for modern smartphones. Multiple-input multiple-output (MIMO) antennas can realize higher data rate and better channel capacity at fixed

power [17]. Thus MIMO, which uses multiple antennas in mobile terminals, is especially important in Wireless Wide Area Network (WWAN) and long-term evolution (LTE) applications [18]–[25]. However, due to strong mutual coupling among closely placed antenna elements, it is a great technical challenge to design a multiband multi-antenna system in small mobile phones. In [20], an LTE MIMO antenna uses an unbroken metallic rim and a non-resonant capacitive coupling element (CCE) respectively as its primary and diversity antenna. The low-loss matching circuit and trapezoidal shaped feed are also utilized to obtain the wide operating bands and good average efficiencies. However, the isolation between the two antennas at higher band is not ideal and the non-ground portions of 10×70 mm^2 are still too large compared with our proposed antenna.

In this paper, a reconfigurable MIMO antenna with integrated metal rim for WWAN/LTE smartphone applications is proposed. The two antenna elements with the same dimensions are centro-symmetrically distributed at the top and bottom edges of the system circuit board. Although the two elements use the same unbroken metal rim as their radiation structure, system ground, and U-shaped feeding line, a better than 17dB isolation between them is achieved. Each element occupies a 30×6 mm^2 ground clearance. The coupled-fed antenna generates four loop resonant modes. Using reconfigurable technique to merge these four loop modes, the proposed antenna can fully cover seven operation bands of GSM850/900/1800/1900/UMTS/LTE2300/2500. The radiation and reconfigurable mechanisms of the proposed antenna are investigated. A prototype of the MIMO antenna is fabricated and characterized. Experimental results are given and discussed.

II. ANTENNA CONFIGURATION

Fig. 1(a) depicts the geometry of the proposed reconfigurable MIMO antenna for WWAN/LTE integrated metal-rimmed smartphones. The front and side views are shown in Figs. 1(b) and 1(c). Fig. 1(d) shows the detailed dimensions of the antenna element. As illustrated in Fig. 1(a), the system circuit board is fabricated on a 0.8 mm thick 145 mm × 72 mm FR4 substrate (ε_r of 4.4 and tanδ of 0.02), which is surrounded by an integrated metal rim of a thickness of 0.3 mm and a height of 6 mm. A ground plane on the bottom side of the FR4 substrate is the system ground. Two non-ground portions of 30 mm × 6 mm are occupied by the U-shaped feed line mounted on the opposite side of the ground to provide a coupled feed. As can be seen in Fig. 1(b), two antenna elements having similar size and configuration, namely, antenna1 and antenna2 are centro-symmetrically placed at the top and bottom edges of the circuit board. Each element comprises a feeding port, a U-shaped feed line, a U-shaped slot located between the metal rim and the system ground, as well as three ON/OFF switches (b, c and d), respectively. To simplify the designing procedure and focus on the working principle of this proposed antenna, the switch is equivalent to an open gap for its OFF state and to a metal strip for its ON state. Fig. 1(c) shows that the distance H_0 between the system ground plane and the backside of the metal rim is 2mm, and the width of the U-shaped slot shown in Fig. 1(d) is 2mm. The position of the three ON/OFF switches are also illustrated in Fig. 1(d), which are located between the system ground plane and the outer metal rim through three narrow strips. When the switches are working in different states (ON or OFF), the antenna operate in different frequency bands.

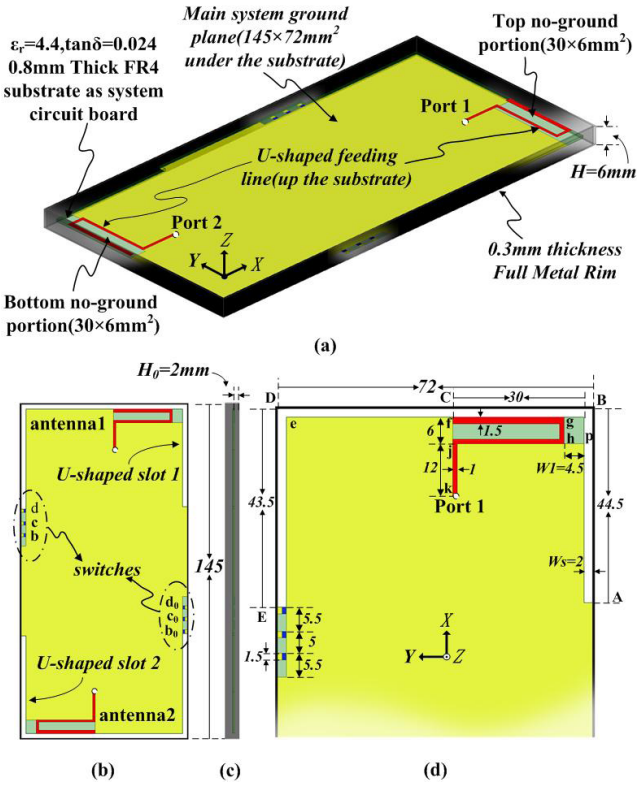

FIGURE 1. Proposed reconfigurable MIMO antenna with integrated metal rim: (a) perspective view; (b) front view; (c) side view; (d) detailed dimensions of the antenna element.

TABLE 1. Reconfigurable mechanism of the proposed antenna.

Frequency band(MHz)		Switch b	Switch c	Switch d	Working state
GSM850	817.8-855.6	OFF	OFF	OFF	A
	851.0-894.2	ON	OFF	OFF	B
GSM900	878.6-920.0	OFF	ON	OFF	C
	919.8-961.2	OFF	OFF	ON	D
GSM1800/ 1900/UMTS	1643-2188	OFF	OFF	OFF	A
LTE2300/ 2500	2150-2780	OFF	OFF	ON	D

III. WORKING PRINCIPLES

To fully comprehend the reconfigurable mechanism of this proposed MIMO antenna, the configurations of the three ON/OFF switches for different working states are shown in TABLE 1. These three switches control the length of the U-shaped metal-loop antenna element to yield four

working states. At each working state, there are four resonant modes which are marked as Mode1 (1-λ), Mode2 (2-λ), Mode3 (1-λ), and Mode4 (3-λ) in sequence from the lower to higher frequencies. In addition, its working mechanism remains unchanged from working states A to D. When all switches (b, c and d) are OFF, marked as state A, the obtained bandwidth of low and high bands can cover 817.8-855.6 MHz and 1643-2188 MHz, respectively. Because of the narrow band of Mode 1 and worsened matching of Mode 4, the antenna working at state A fails to meet the required bands (824-960 and 1710-2170 MHz). When the switch b is ON and the others are OFF, marked as state B, the achieved bandwidth in low band can provide coverage for 851-894.2 MHz. When the switch c is ON and the other switches are OFF, marked as state C, the obtained bandwidth in low band can cover 878.6-920MHz. When the switch d is ON and the others are OFF, marked as state D, the achieved bandwidth of low and high bands can cover 919.8-961.2 MHz and 2150-2780 MHz, respectively. Hence, this proposed reconfigurable MIMO antenna can cover 824-960 MHz and 1710-2690 MHz by merging states A, B, C and D in low band and states A and D in high band, respectively.

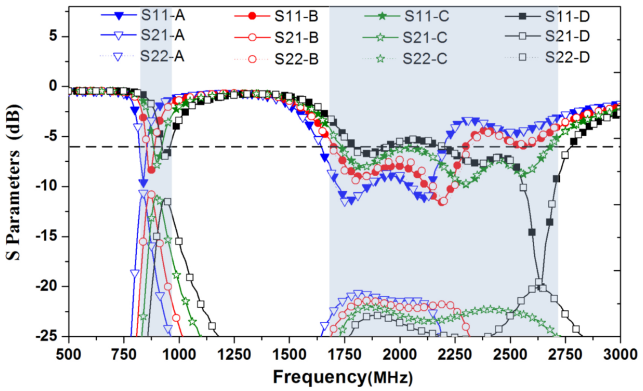

FIGURE 2. Simulated S parameter of the proposed antenna for four working states (states A, B, C, and D).

Fig. 2 shows the simulated S parameter of the proposed antenna for four working states (states A, B, C, and D) using HFSS version 15. As can be seen in Fig. 2, the simulated 6 dB impedance bandwidth (across 3:1 VSWR) can cover the desired seven-band WWAN/LTE operations. Owing to the same dimension and centrosymmetric placement for both two antenna elements, the simulated S11 and S22 are quite similar. Meanwhile, the simulated isolations in the low band of 824-960 MHz and high band of 1710-2170 MHz are larger than 11 dB and 20 dB, respectively. This is because the lower frequency of 1-wavelength resonant mode is excited by the outermost U-shaped metal loop plotted in Fig. 1(d). When the two antenna elements sharing the same unbroken metal rim work in the lower resonant frequency, the current strength in the metal loop is stronger than that in the higher resonant frequency. Even though the coupling current between two elements in lower frequency is stronger, the isolation in low band is still to be above 11 dB. The reason is that the current is mostly concentrated in the metal loop when a loop antenna works. Good isolation can be achieved if the distance between two loop antenna elements is far enough. Hence, the proposed loop antenna can be easily integrated into the outer metal rim as part of antenna, but it also provides good isolation between MIMO antenna elements sharing the same unbroken metal rim.

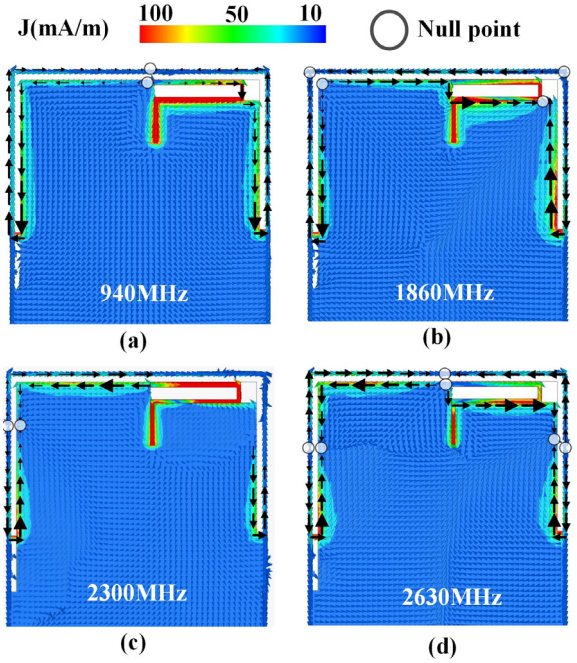

FIGURE 3. Typical surface vector current distributions for the proposed antenna element at D state: (a) 940 MHz; (b) 1860 MHz; (c) 2300 MHz; and (d) 2630 MHz.

To understand the resonant mechanism for this proposed antenna, the simulated surface vector current distributions at 940, 1860, 2300 and 2630 MHz are shown in Fig. 3. For sake of brevity, state D is chosen for the evaluation (the switch d is ON and the other switches are OFF). As can be seen from Fig. 3(a), two current nulls at 940 MHz are found along the coupling loop antenna consisting of a part of metal rim, the system ground and the U-shaped feeding line. This means that Mode 1 is its fundamental loop mode (1-λ loop mode). Similarly, the other two high-order loop modes of Mode 2 (2-λ loop mode) and Mode 4 (3-λ loop mode) can be comprehended clearly after analyzing the corresponding current distributions illustrated in Figs. 3(b) and (d), respectively. By observing Fig. 3(c), the surface current is mainly distributed in the left metal loop at 2300 MHz. A 1λ coupling loop mode (Mode3) is excited. Moreover, some weak currents are induced in the right metal loop in a manner that is similar to that of a matching circuit of shunt inductance, which improves the impedance matching.

In order to explain the effects of the parameters to antenna performances, a key parameter L2, which is the length of the U-shaped feeding line, is studied. Fig. 4 shows the

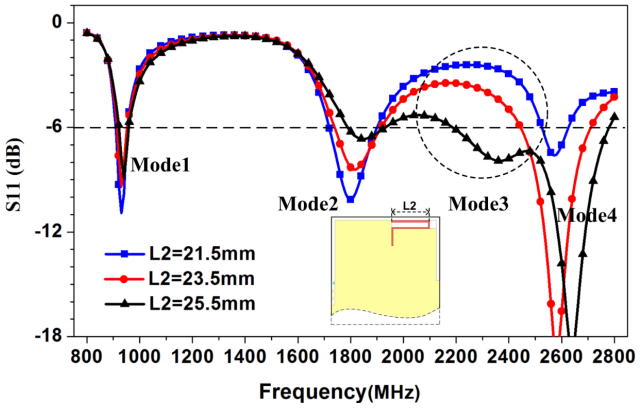

FIGURE 4. Simulated S11 for the antenna element at D state as a function of L2.

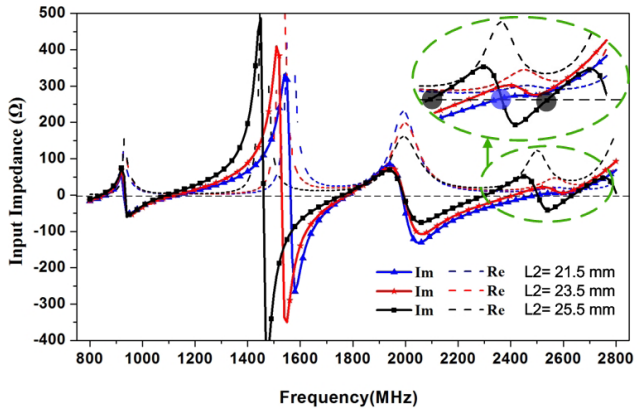

FIGURE 5. Simulated input impedances for the antenna element at D state as a function of L2.

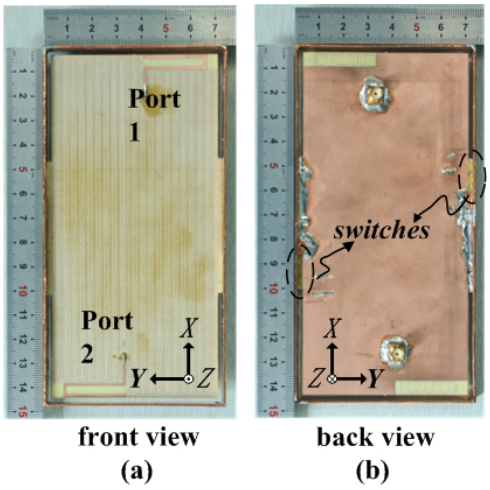

FIGURE 6. Photographs of the fabricated prototype (a) front view (b) back view.

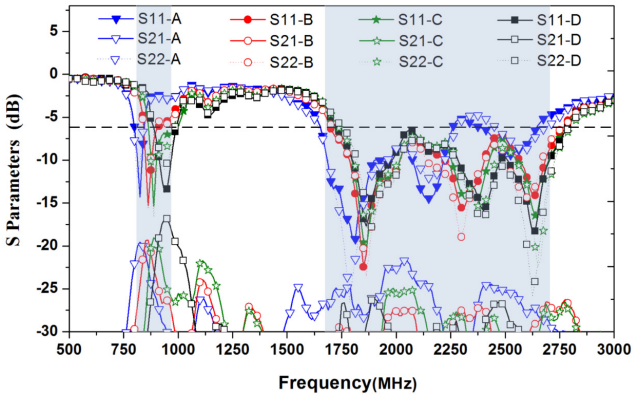

FIGURE 7. Measured S parameters of the proposed MIMO antenna.

simulated S11 for the antenna element working at D state as a function of L2. When the length of L2 is increased from 21.5 to 25.5 mm, the number of the resonant modes in higher frequency vary from two (Modes 2 and 4) to three (Modes 2, 3 and 4). To analyze the causes, simulated input impedances of the antenna element for different values of L2 are shown in Fig. 5. When L2 = 21.5 mm, it can be observed that there are two zero reactances in ∼1800 MHz and ∼2500 MHz, which indicates that two resonant modes occur in the high band. However, when L2 = 25.5mm, there are three resonant modes generated in ∼1800 MHz, ∼2300 MHz and ∼2630 MHz, respectively. By comparing the input impedance in these two different conditions, it is obvious that a new resonance mode (mode 3 or ∼2300 MHz) in the high band is obtained. This is because the energy coupling between the feeding line and the left metal rim becomes stronger when the length of L2 increases and mode 3 is excited.

IV. MEASUREMENT AND DISCUSSION

The proposed antenna has been fabricated as shown in Fig. 6. The performance measurement is characterized using an Agilent N5247A vector network analyzer and the radiation performances are obtained in the SATIMO microwave anechoic chamber. A 50Ω SMA connector is connected to the feeding port for exciting the antenna. Fig. 7 shows the measured S parameters for the prototype which shows good agreement with the simulated ones plotted in Fig. 2. The difference is that measured isolation is above 17 dB in the lower band, which is better than the simulated isolation. Moreover, when the antenna works at C or D state, the lower frequency bandwidth is wider than that in the simulated result.

The measured total efficiency and gain conducted with one antenna element measured and another antenna element terminated to 50-Ω loads are presented in Fig. 8. For the lower bands of 824–960 MHz, the antenna gain variation is from -0.32 to 1.4 dBi and the total efficiency is more than 43%, indicating great promises in practical smartphone applications. For the higher bands of 1710–2690 MHz, the achieved antenna gain is about 1.6–4.8 dBi with the corresponding total efficiency of approximately 59–72%. Therefore, the measured radiation performances of this antenna over the whole operating bands can meet the demands for smartphone systems.

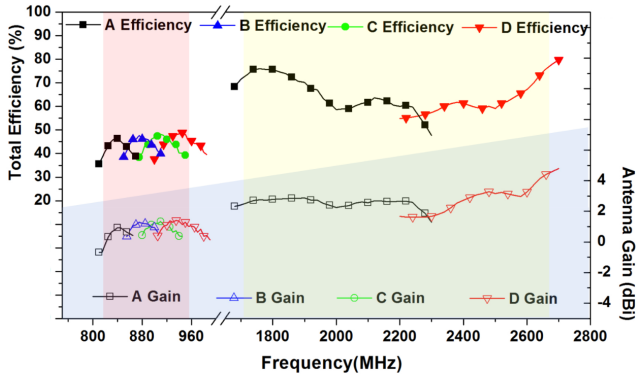

FIGURE 8. Measured total efficiency and gain for the fabricated antenna for four working states.

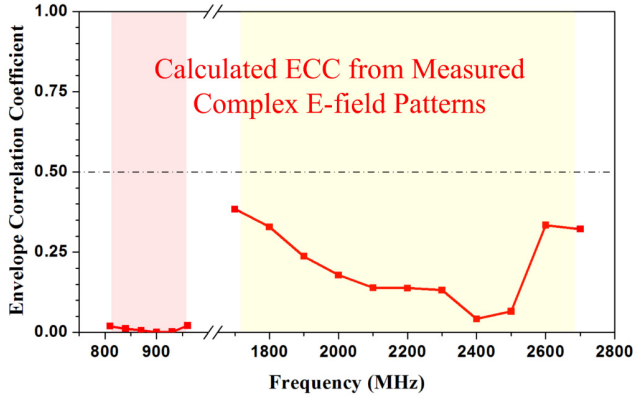

FIGURE 9. Calculated ECC from the measured complex E-field patterns.

TABLE 2. Diversity performance of the proposed antenna array.

Frequency (MHz)	850	900	950	1800
ECC	0.01	0.00	0.02	0.33
MEG1 (dB)	-9.8	-9.6	-9.7	-5.1
MEG2 (dB)	-9.1	-9.1	-9.3	-4.8
Frequency (MHz)	2000	2200	2400	2600
ECC	0.18	0.14	0.04	0.34
MEG1 (dB)	-4.8	-4.2	-3.8	-4.4
MEG2 (dB)	-4.6	-4.5	-3.7	-4.2

The potential MIMO performance of this proposed antenna is evaluated by calculating the envelop correlation coefficient (ECC), mean effective gain (MEG), as well as channel capacity. The ECC in Fig. 9 and the MEG in Table 2 are calculated from the measured complex E-field patterns of the fabricated MIMO antenna. As can be seen from Fig. 9, the ECC values in the lower band and upper bands are less than 0.02 and 0.4, respectively, which means low correlation and good diversity performance. As can be observed from Table 2, the proposed MIMO antenna can achieve $|\text{MEG1} - \text{MEG2}| < 1\text{dB}$ within the entire operating bands, which indicates that it is suitable for practical smartphone MIMO antenna applications. Furthermore, the calculated ergodic channel capacities of the fabricated

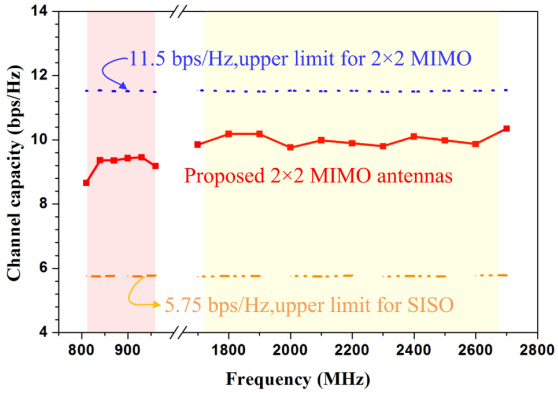

FIGURE 10. Calculated ergodic channel capacities of the fabricated 22 MIMO antennas.

22 MIMO antennas is represented in Fig. 10. As can be seen, the channel capacities in the lower and higher bands are about 9 bps/Hz and 10 bps/Hz, respectively.

V. CONCLUSION

A reconfigurable MIMO antenna was designed and analyzed in this paper for WWAN/LTE integrated-metal- rimmed smartphone applications. Although the two loop antenna elements use the same unbroken metal rim as well as their radiation structure, a good isolation of better than 17dB over the entire operating bands is achieved. By combining four typical loop modes, this antenna can cover seven operation bands of GSM850/900/1800/1900/UMTS/LTE2300/2500 with the help of reconfigurable technique and coupled feed manner. The proposed reconfigurable MIMO antennas were designed, fabricated and characterized. Encouraging results regarding S-parameters, antenna efficiency and gain, ECC, MEG, along with ergodic channel capacity are obtained, and found to meet the contemporary needs of smartphone applications. As such, the proposed reconfigurable antenna is recommended for smartphones applications with WWAN and LTE operations.

REFERENCES

[1] R. S. Aziz, A. K. Arya, and S.-O. Park, "Multiband full-metal-rimmed antenna design for smartphones," *IEEE Antennas Wireless Propag. Lett.*, vol. 15, pp. 1987–1990, 2016.

[2] Q. Guo, R. Mittra, F. Lei, Z. Li, J. Ju, and J. Byun, "Interaction between internal antenna and external antenna of mobile phone and hand effect," *IEEE Trans. Antennas Propag.*, vol. 61, no. 2, pp. 862–870, Feb. 2013.

[3] Y. Liu, Y.-M. Zhou, G.-F. Liu, and S.-X. Gong, "Heptaband inverted-F antenna for metal-rimmed mobile phone applications," *IEEE Antennas Wireless Propag. Lett.*, vol. 15, pp. 996–999, 2016.

[4] K.-L. Wong and Y.-C. Wu, "Small-size dual-wideband IFA frame antenna closely integrated with metal casing of the LTE smartphone and having decreased user's hand effects," *Microw. Opt. Technol. Lett.*, vol. 58, no. 12, pp. 2853–2858, Dec. 2016.

[5] J. W. Lian, Y.-L, Ban, Y.-L. Yang, L.-W. Zhang, C.-Y.-D. Sim, and K. Kang, "Hybrid multi-mode narrow-frame antenna for WWAN/LTE metal-rimmed smartphone applications," *IEEE Access*, vol. 4, pp. 3991–3998, 2016.

[6] Y. L. Ban, Y. F. Qiang, Z. Chen, K. Kang, and J. H. Guo, "A dual-loop antenna design for hepta-band WWAN/LTE metal-rimmed smartphone applications," *IEEE Trans. Antennas Propag.*, vol. 63, no. 1, pp. 48–58, Jan. 2015.

[7] C.-K. Hsu and S.-J. Chung, "Compact multiband antenna for handsets with a conducting edge," *IEEE Trans. Antennas Propag.*, vol. 63, no. 11, pp. 5102–5107, Nov. 2015.
[8] D. Wu, S. W. Cheung, and T. I. Yuk, "A compact and low-profile loop antenna with multiband operation for ultra-thin smartphones," *IEEE Trans. Antennas Propag.*, vol. 63, no. 6, pp. 2745–2750, Jun. 2015.
[9] D. Wu, S. W. Cheung, and T. I. Yuk, "Compact 3D-loop antenna with bandwidth enhancement for WWAN/LTE mobile-phones applications," *IET Microw., Antennas Propag.*, vol. 11, no. 2, pp. 240–246, Jan. 2017.
[10] H. Xu *et al.*, "A compact and low-profile loop antenna with six resonant modes for LTE smartphone," *IEEE Trans. Antennas Propag.*, vol. 64, no. 9, pp. 3743–3751, Sep. 2016.
[11] J.-H. Lu and F.-C. Tsai, "Planar internal LTE/WWAN monopole antenna for tablet computer application," *IEEE Trans. Antennas Propag.*, vol. 61, no. 8, pp. 4358–4363, Aug. 2013.
[12] H.-B. Zhang, Y.-L. Ban, Y.-F. Qiang, J. Guo, and Z.-F. Yu, "Reconfigurable loop antenna with two parasitic grounded strips for WWAN/LTE unbroken-metal-rimmed smartphones," *IEEE Access*, vol. 5, pp. 4853–4858, 2017.
[13] Y. Li, Z. Zhang, J. Zheng, Z. Feng, and M.-F. Iskander, "A compact hepta-band loop-inverted F reconfigurable antenna for mobile phone," *IEEE Trans. Antennas Propag.*, vol. 60, no. 1, pp. 389–392, Jan. 2012.
[14] Y. Xu, Y.-W. Liang, and H.-M. Zhou, "Small-size reconfigurable antenna for WWAN/LTE/GNSS smartphone applications," *IET Microw., Antennas Propag.*, vol. 11, no. 6, pp. 923–928, May 2017.
[15] Y. K. Park and Y. Sung, "A reconfigurable antenna for quad-band mobile handset applications," *IEEE Trans. Antennas Propag.*, vol. 60, no. 6, pp. 3003–3006, Jun. 2012.
[16] Y.-L. Ban, Q.-F. Qiang, G. Wu, H. Wang, and K.-L. Wong, "Reconfigurable narrow-frame antenna for LTE/WWAN metal-rimmed smartphone applications," *IET Microw., Antennas Propag.*, vol. 10, no. 10, pp. 1092–1100, 2016.
[17] K.-L. Wong, C.-Y. Tsai, and J.-Y. Lu, "Two asymmetrically mirrored gap-coupled loop antennas as a compact building block for eight-antenna MIMO array in the future smartphone," *IEEE Trans. Antennas Propag.*, vol. 65, no. 4, pp. 1765–1778, Apr. 2017.
[18] L. Y. Qu *et al.*, "MIMO antennas using controlled orthogonal characteristic modes by metal rims," *IET Microw., Antennas Propag.*, vol. 11, no. 7, pp. 1009–1015, 2016.
[19] P.-W. Lin and K.-L. Wong, "Dual-feed small-size LTE/WWAN strip monopole antenna for tablet computer applications," *Microw. Opt. Technol. Lett.*, vol. 55, no. 11, pp. 2571–2576, Nov. 2013.
[20] M. Stanley, Y. Huang, H. Wang, S. S. Alja'afreh, Q. Xu, and L. Xing, "LTE MIMO antenna using unbroken metallic rim and non resonant CCE element," in *Proc. Eur. Conf. Antennas Propag. (EuCAP)*, Davos, Switzerland, Apr. 2016, pp. 1–4.
[21] S. Wang and Z. Du, "A multiband dual-antenna system with a folded fork-shaped ground branch and folded asymmetric U-Shaped slots for smartphone applications," *IEEE Antennas Wireless Propag. Lett.*, vol. 14, pp. 1626–1629, 2015.
[22] K.-L. Wong, Y.-C. Chen, and W.-Y. Li, "Four LTE low-band smartphone antennas and their MIMO performance with user's hand presence," *Microw. Opt. Technol. Lett.*, vol. 58, no. 9, pp. 2046–2052, Sep. 2016.
[23] K.-L. Wong, T.-W. Kang, and M.-F. Tu, "Internal mobile phone antenna array for LTE/WWAN and LTE MIMO operations," *Microw. Opt. Technol. Lett.*, vol. 53, no. 7, pp. 1569–1573, Jul. 2011.
[24] K. Zhao, S. Zhang, K. Ishimiya, Z. Ying, and S. He, "Body-insensitive multimode MIMO terminal antenna of double-ring structure," *IEEE Trans. Antennas Propag.*, vol. 63, no. 5, pp. 1925–1936, May 2015.
[25] J. Anguera, A. Andújar, and C. García, "Multiband and small coplanar antenna system for wireless handheld devices," *IEEE Trans. Antennas Propag.*, vol. 61, no. 7, pp. 3782–3789, Jul. 2013.

ZI-QIANG XU (M'13), photograph and biography not available at the time of publication.

YANG-TAO SUN, photograph and biography not available at the time of publication.

QIANG-QIANG ZHOU, photograph and biography not available at the time of publication.

YONG-LING BAN, photograph and biography not available at the time of publication.

YUAN-XUN LI, photograph and biography not available at the time of publication.

SIMON S. ANG (S'79–M'79–SM'94–F'11), photograph and biography not available at the time of publication.